







Evaluation of lumican effects on morphology of invading breast cancer cells, expression of integrins and downstream signaling

Konstantina Karamanou^{1,2,3} , Marco Franchi⁴ , Maurizio Onisto⁵ , Alberto Passi⁶ ,
Demitrios H. Vynios¹  and Stéphane Brézillon^{2,3} 

- 1 Biochemistry, Biochemical Analysis & Matrix Pathobiology Research Group, Laboratory of Biochemistry, Department of Chemistry, University of Patras, Greece
- 2 Laboratoire de Biochimie Médicale et Biologie Moléculaire, Université de Reims Champagne-Ardenne, France
- 3 Matrice Extracellulaire et Dynamique Cellulaire, CNRS UMR 7369, Reims, France
- 4 Department for Life Quality Studies, University of Bologna, Rimini, Italy
- 5 Department of Biomedical Sciences, University of Padua, Italy
- 6 Department of Surgical and Morphological Sciences, University of Insubria, Varese, Italy

Keywords

breast cancer; integrins; invadopodia;
lumican; proteoglycans

Correspondence

S. Brézillon, Matrice Extracellulaire et
Dynamique Cellulaire (MEDyC), CNRS UMR
n°7369, Université de Reims Champagne-
Ardenne, 51 rue Cognacq Jay, Reims
51095, France
Tel: + 33 3 26 91 37 34
E-mail: stephane.brezillon@univ-reims.fr

(Received 6 June 2019, revised 11 October
2019, accepted 9 March 2020)

doi:10.1111/febs.15289

The small leucine-rich proteoglycan lumican regulates estrogen receptors (ERs)-associated functional properties of breast cancer cells, expression of matrix macromolecules, and epithelial-to-mesenchymal transition. However, it is not known whether the ER-dependent lumican effects on breast cancer cells are related to the expression of integrins and their intracellular signaling pathways. Here, we analyzed the effects of lumican in three breast cancer cell lines: the highly metastatic ER β -positive MDA-MB-231, cells with the respective ER β -suppressed (shER β MDA-MB-231), and lowly invasive ER α -positive MCF-7/c breast cancer cells. Scanning electron microscopy, confocal microscopy, real-time PCR, western blot, and cell adhesion assays were performed. Lumican effects on breast cancer cell morphology were also investigated in 3-dimensional collagen cultures. Lumican treatment induced cell-cell contacts and cell grouping and inhibited microvesicles and microvilli formation. The expression of the cell surface adhesion receptor CD44, its isoform and variants, hyaluronan (HA), and HA synthases was also investigated. Lumican inhibited the expression of CD44 and HA synthases, and its effect on cell adhesion revealed a major role of $\alpha 1$, $\alpha 2$, $\alpha 3$, $\alpha V\beta 3$, and $\alpha V\beta 5$ integrins in MDA-MB-231 cells, but not in MCF-7/c cells. Lumican upregulated the expression of $\alpha 2$ and $\beta 1$ integrin subunits both in MDA-MB-231 and in shER β MDA-MB-231 as compared to MCF-7/c cells. Downstream signaling pathways for integrins, such as FAK, ERK 1/2 MAPK 42/44, and Akt, were found to be downregulated by lumican. Our data shed light to the molecular mechanisms responsible for the anticancer activity of lumican in invasive breast cancer.

Abbreviations

As, anti-sense; CD44, cluster of differentiation 44; CD44s, CD44 (standard isoform); ECM, extracellular matrix; EGFR, epidermal growth factor receptor; EMT, epithelial-to-mesenchymal transition; ERK, extracellular-related kinase; FAK, focal adhesion kinase; HA, hyaluronic acid; KS, keratan sulfate; LRR, leucine-rich repeat; MAPK, mitogen-activated protein kinases; MMP, matrix metalloproteinase; MT1-MMP, membrane type 1-matrix metalloproteinase; PG, proteoglycan; SLRP, small leucine-rich proteoglycans.

Introduction

Breast cancer is a major research field, as it is the predominant type of cancer among women with 25% of cancer cases to be identified as breast cancer incidents [1]. A great hallmark of breast cancer is the absence or presence of estrogen receptors alpha and beta (ER α and ER β). Estrogens are a hormonally active family, having a major role in several cellular functions of breast cancer and being related to the expression of matrix macromolecules, and therefore with the cell–cell and cell–extracellular matrix interactions [2,3]. There are two different estrogen receptors, in terms of genetics, structure, and, therefore, functionality, the ER α and ER β [4]. ER α is considered to be the most important subtype in the mammary epithelium, and therefore, it is considered as a prognostic marker for breast cancer incidents. ER α is fertile ground for pharmaceutical targeting of breast cancer, since the 17 β -estradiol (E2)/estrogen receptor alpha (ER α) signaling is of pivotal importance, as it features 70% of breast cancer cases as ER α -positive [5]. Although most ER α -positive tumors respond initially to anti-estrogenic therapies, that is, tamoxifen, they end up resistant independently of the ER status and they potentially result in endometrial carcinoma [6]. Therefore, it is regarded as fundamental to investigate new therapies, with less side effects and higher specificity to the target cell.

Although the biological activity of ER α is extensively explored, its ER β isoform is less investigated. It is reported that when ER β is being activated, it potentially forms heterodimers with ER α , and therefore affects the biological functions of ER α , too [7,8]. It was recently reported that the triple-negative, but ER β -positive, MDA-MB-231 breast cancer cells [9,10], when transfected with shRNA against human ER β , ER β mRNA was suppressed by 70% triggering major alterations in cell functions of the aggressive breast cancer cells, as well as in the epithelial-to-mesenchymal (EMT) markers, leading to a potent mesenchymal-to-epithelial transition (MET) situation. The ER β -suppressed MDA-MB-231 cells present an epithelial-like phenotype, more cell–cell adhesion junctions, upregulation of the expression of epithelial markers, like E-cadherin, and downregulation of the mesenchymal ones, like vimentin and fibronectin. EMT and MET were shown to occur in healing and metastasis, so we took advantage of it and we aimed at identifying new molecular players.

Mesenchymal cells possess the ability to migrate and invade due to the formation of invasive protrusions, the invadopodia, whereas in epithelial cells, lamellipodia and filopodia are mostly found [11,12]. Invadopodia are

characterized as tightly packed, organelle-free, actin-rich protrusions of the plasma membrane, playing a governing role in the steps of metastasis, from invasion to the neighboring stroma, intravasation, and finally extravasation [13,14]. Cytoskeletal changes at invadopodia are monitored by cortactin, and extracellular matrix (ECM)-degrading function of invadopodia is determined by membrane type-1–matrix metalloproteinase (MT1-MMP or MMP-14); therefore, cortactin and MMP-14 are two major proteins governing the invadopodia formation. Cortactin is reported to be overexpressed by 13% of breast carcinomas, and its overexpression enhances cell migration, invasion, and tumor cell metastasis, whereas when it is blocked, the Src signaling is thereafter blocked, leading to the inhibition of invadopodia formation [15–20]. It is also worth noticing that cortactin is essential for the maintenance of F-actin-enriched invadopodia core structures, as well as for the initiation and sustainability of matrix degradation, in cooperation with MMP-14. Integrins are considered to bind and activate MMPs, through which they regulate the effective invasion of invadopodia into the extracellular matrix. It has been observed that β 1 integrin coclusters with MMP-14 at sites of interaction with collagen fibers along the cell leading edge, and therefore, the adhesive mechanism is involved in invadopodia maturation and ECM degradation [21].

Vinculin is a governing protein in several cell functions, such as cell adhesion, cell migration, and embryonic development, since it has the ability to interact with integrins to the cytoskeleton at the focal adhesions [22–25]. Therefore, vinculin is a fundamental marker of cell–cell junctions and focal adhesion, located in the periphery of newly created invadopodia. Consequently, the downregulation of vinculin prevents or inhibits several cellular functions, such as cell adhesion, formation of focal adhesions, as well as lamellipodia protrusions [26], whereas its overexpression facilitates cell adhesion and recruitment of cytoskeletal proteins at the domains of integrin binding at the focal adhesions [27,28].

Cancer progression and metastasis occur during constant-specific interactions between cancer cells and their microenvironment, and ECM is responsible for the signaling of those interactions. Proteoglycans (PGs) are multifunctional effectors of the ECM and are implicated in pathophysiological processes. Their expression is significantly altered during cancer progression, and their modulated exposure on the tumor ECM and tumor cell membranes affects a plethora of cellular functions [29,30]. The most abundantly expressed PGs in ECM are the small leucine-rich proteoglycans (SLRPs), which are able to interact with

matrix effectors, such as cytokines, growth factors, and cell surface proteins, and consequently regulate the cell functional features, such as migration, autophagy, angiogenesis, and metastasis [31–34]. Lumican, a class II SLRP, expressed as a major KSPG in cornea. It is also worth noticing that lumican presents high molecular heterogeneity according to the tissue due to its glycosylation [35]. Structurally, lumican consists of 18 amino acid signal peptide and three major domains of (–) charged N-terminal domain (Tyr sulfates and cysteine residues), a central part containing nine LRRs and a C-terminal domain of 66 amino acids (two conserved cysteine residues and two leucine-rich repeats) [36,37]. Although there are several reports concerning the anticancer effect of lumican, the underlying mechanism is not totally identified. The anticancer effect of lumican may be due to the direct binding of $\alpha 2\beta 1$ integrin, which stimulates cell adhesion and inversely inhibits cell migration [38]. The interaction of lumican with integrins can also be associated with TGF- $\beta 2$, since altered expression of TGF- $\beta 2$ was found to be accompanied by downstream modification of the signaling transduction of pSMAD2 and increased activity of $\beta 1$ integrin [39]. It is also reported that when lumican interacts with integrins, it inhibits cell migration metastasis and EMT [40]. When lumican interacts with TGF- β , the binding of TGF- β to its respective receptors is altered and consequently cell adhesion and metastasis are affected. It is also reported that lumican induces phagocytosis through interaction with CD14, regulates immune response through interaction with TLR4, as well as to be implicated in apoptosis and immune response by interacting with Fas-Fas ligand [34,35].

It was recently published that lumican significantly attenuates cell functional properties, such as cell growth, migration, and invasion; it modifies cell morphology, so as cell–cell junctions, and evokes EMT/MET by reprogramming and suppressing the expression of major matrix effectors implicated in breast cancer progression [41]. However, the mechanism lying behind the anticancer effect of lumican remains unclear. Thus, the aim of this study was to evaluate whether the ER-dependent lumican effects in breast cancer cells are related to the expression of integrins and the intracellular signaling pathways related to matrix effectors. Specifically, the effects of lumican on the morphology of highly metastatic cancer cells, and the expression of integrins and downstream signaling pathways were investigated. The ER α -positive and low aggressive MCF-7/c, ER α -negative and ER β -positive MDA-MB-231, and the shER β MDA-MB-231 breast cancer cells were used. The obtained data reveal a

novel role of metastasis-implicated molecules in the anticancer effect of lumican.

Results

Lumican effects on cell morphology of invading MDA-MB-231 breast cancer cells in collagen substrate after 24 and 48 h

Highly invasive MDA-MB-231 breast cancer cells were seeded on a Millipore[®] (Milan, Italy) filter coated with type I collagen for 24 h and observed at the scanning electron microscopy (SEM). Cells showed different isolated phenotypes: globular cells, and elongated and spindle-like shaped cells exhibiting microvesicles and cytoplasmic protrusions like filopodia, lamellipodia, and invadopodia [Fig. 1A (a)]. In regions of the Millipore filter where collagen coating was thicker, MDA-MB-231 cells, completely covered by microvesicles, invaginated the collagen sheet which contained isolated microvesicles mainly shed by globular-shaped cells [Fig. 1A (b, c)]. After treatment with 100 nM lumican for 24 h in serum-free conditions and seeding on the surface of a Millipore[®] filter coated with collagen type I, MDA-MB-231 cells showed the same shapes, but appeared more flattened, and most of them displayed a smoother surface with less cytoplasmic protrusions, and fewer microvilli and microvesicles in comparison with untreated cells. Moreover, both globular and elongated cells were often in cell–cell contact [Fig. 1A (d, e, f)]. SEM analysis was also performed on MDA-MB-231 cells seeded for 48 h with and without lumican treatment. The untreated MDA-MB-231 cells appeared more globular as compared to those cultured for 24 h but still showed cytoplasmic microvesicles and microvilli. Few flattened cells with microvesicles displaying many invadopodia or thicker cytoplasmic protrusions in direct contact with collagen fibrils were also present [Fig. 1A (g, h, i)]. The same cells treated with 100 nM lumican showed only globular shape, appeared more grouped, and exhibited less microvesicles than untreated cells. No invadopodia or lamellipodia were detectable, and some of them even showed a very smooth surface being completely devoid of microvesicles or displayed only few microvilli [Fig. 1A (j, k, l)].

Lumican induces morphological alterations of MCF-7/c breast cancer cells during invasion in collagen substrate after 24 and 48 h

Low-invasive MCF-7/c breast cancer cells seeded on Millipore[®] filters coated with type I collagen for 24 h and observed at SEM mainly showed polygonal shape.

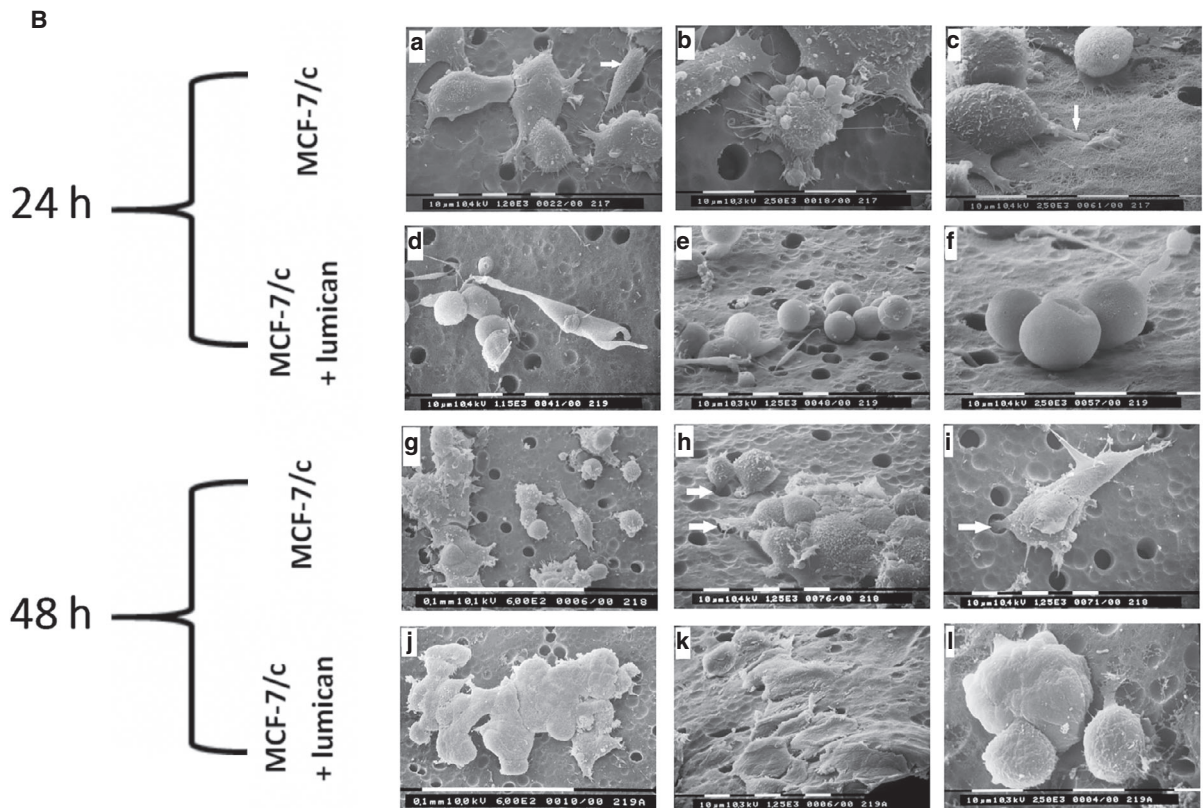
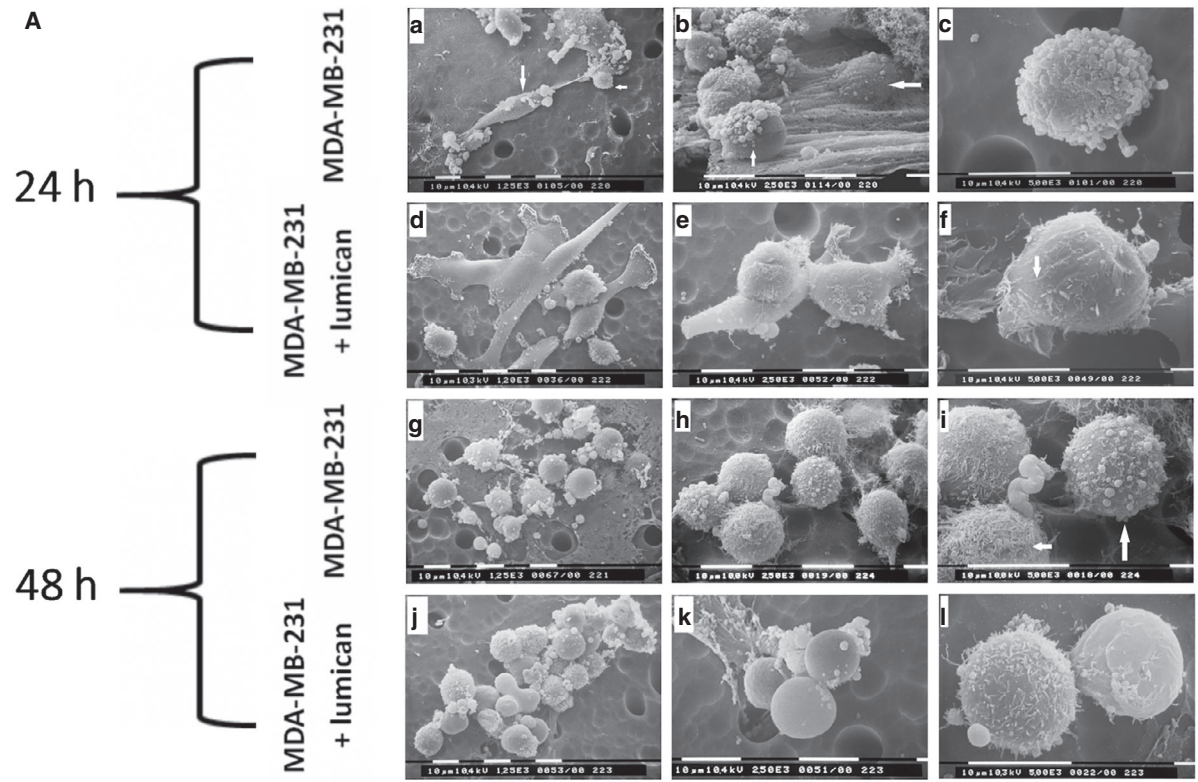


Fig. 1. Evaluation of cell morphology in breast cancer cells invading a collagen coating. (Experiment was twice repeated, and each trial included four samples for each group). (A) Observation of MDA-MB-231 cells seeded on the Millipore® filter coated with type I collagen. SEM pictures of highly invasive MDA-MB-231 breast cancer cells seeded for 24 h on a Millipore® filter coated with type I collagen show different phenotypes: a small globular cell exhibiting microvesicles (small arrow), an elongated cell, and a spindle-like shaped one with filopodia (large arrow). Scale bar = 10 µm (image a). Thick collagen coating partially or completely (large arrow) covers globular cells rich in microvesicles (small arrow). Scale bar = 10 µm (image b). An isolated globular cell is completely coated with microvesicles. Scale bar = 10 µm (image c). After treatment with 100 nm lumican globular, flattened and elongated cells in cell–cell contact show a smooth cytoplasmic surface with very few microvesicles and few microvilli. Scale bar = 10 µm (images d and e). A globular cell exhibits only few microvilli (arrow). Scale bar = 10 µm (image f). SEM pictures of MDA-MB-231 cells seeded for 48 h on a Millipore® filter coated with type I collagen: Most of the cells appear globular-like and show microvesicles. Scale bar = 10 µm (image g). Globular cells with microvesicles (large arrow) and microvilli (small arrow). Scale bar = 10 µm (images h and i). After 100 nm lumican treatment, cells appear like grouped-globular cells at SEM: Some of them show few microvesicles but others exhibit a smooth surface with no microvesicles. Scale bar = 10 µm (image j). Three grouped very smooth globular cells with almost no microvesicles and no microvilli are in direct contact with a collagen sheet. Scale bar = 10 µm (image k). Two globular cells show only microvilli (on the left) and very few cytoplasmic protrusions (on the right). Scale bar = 10 µm (image l). (B) Cell morphology of low-invasive MCF-7/c breast cancer cells seeded on a Millipore® filter coated with type I collagen. Cells seeded for 24 h and observed at SEM show polygonal grouped cells in cell–cell contact with few microvesicles and microvilli. An isolated elongated cell with cytoplasmic protrusions is also detectable on the right. Scale bar = 10 µm (arrow, image a). A globular cell, a flattened and an elongated one, exhibits both microvesicles and microvilli. Scale bar = 10 µm (image b). Cells displaying microvilli show invadopodia (arrow) in direct contact with collagen network. Scale bar = 10 µm (image c). MCF 7/c cells after treatment with 100 nm lumican: Both globular grouped cells and isolated fusiform cells show a very smooth surface. Scale bar = 10 µm (images d and e). Three completely smooth globular grouped cells show very few microvilli but no microvesicles. Scale bar = 10 µm (image f). MCF-7/c breast cancer cells seeded on a Millipore® filter coated with type I collagen for 48 h and then observed at SEM show grouped polygonal and globular cells in cell–cell contact with few microvesicles and microvilli, but also isolated globular cells and an elongated one with invadopodia are detectable. Scale bar = 0.1 mm (image g). Grouped polygonal cells and two globular ones with microvilli and invadopodia are migrating through the holes of Millipore® filter (arrows). Scale bar = 10 µm (image h). An isolated elongated cell with invadopodia (arrow) is passing through the holes of the filter. Scale bar = 10 µm (image i). After 48 h, 100 nm lumican treatment grouped flattened polygonal and globular cells in a very tight contact with almost no microvesicles or microvilli are detectable. Scale bar = 0.1 mm (image j). Cells treated with lumican show flattened polygonal cells in tight contact to each other with no invadopodia, no microvesicles, almost absent microvilli, and very few cytoplasmic protrusions. Scale bar = 10 µm (image k). Grouped flattened and globular cells with no microvesicles nor microvilli are detectable. Scale bar = 10 µm (image l).

Cells were grouped with cell–cell junctions, even though few elongated or fusiform-shaped cells were also detectable. Some cells displayed cytoplasmic protrusions, but all cells exhibited few microvilli and few microvesicles [Fig. 1B (a, b)]. In areas where collagen network was thicker, cells presented lamellipodia and invadopodia in tight contact with collagen fibrils and displayed many microvilli [Fig. 1B (c)]. The same cells treated with 100 nm lumican and observed at SEM after 24 h showed mainly globular-shaped cells in cell–cell contacts with no lamellipodia and invadopodia. However, many of them showed an extremely smooth cytoplasmic surface with no microvilli or microvesicles, even in the elongated/fusiform ones [Fig. 1B (d, e, f)]. Untreated MCF-7/c cells observed after 48 h mainly showed grouped polygonal- and globular-shaped cells in cell–cell contacts with few microvesicles and microvilli on the cytoplasmic surface [Fig. 1B (g, h)]. However, few elongated cells with invadopodia were also detectable [Fig. 1B (i)]. After the 100 nm lumican treatment, the same cells displaying polygonal and globular shapes appeared more grouped, more flattened, and in very tight contact to each other. Lumican-treated MCF-7/c showed tight cell–cell contact,

decreased number of cytoplasmic microvilli, no microvesicles, and no lamellipodia or invadopodia in comparison with untreated cells [Fig. 1B (j, k, l)].

Lumican affects the expression levels of invadopodia markers and focal adhesion proteins in breast cancer cells

Taking into account that invadopodia are membrane protrusions of invasive cancer cells, which mediate focal pericellular degradation of ECM and play a governing role in tumor development, cellular invasion, and metastasis, the effect of lumican on the expression of invadopodia markers was examined in breast cancer cell lines.

The distribution of cortactin was analyzed by immunofluorescence (Fig. 2A).

In MDA-MB-231 cells, actin–cortactin aggregates were observed, indicating the initiation of invadopodia formation. On the contrary, in the presence of lumican, the expression of cortactin was decreased and accompanied by strong inhibition of cytoplasmic and pericellular staining (Fig. 2A, arrows). These results indicated that cortactin was required for the formation

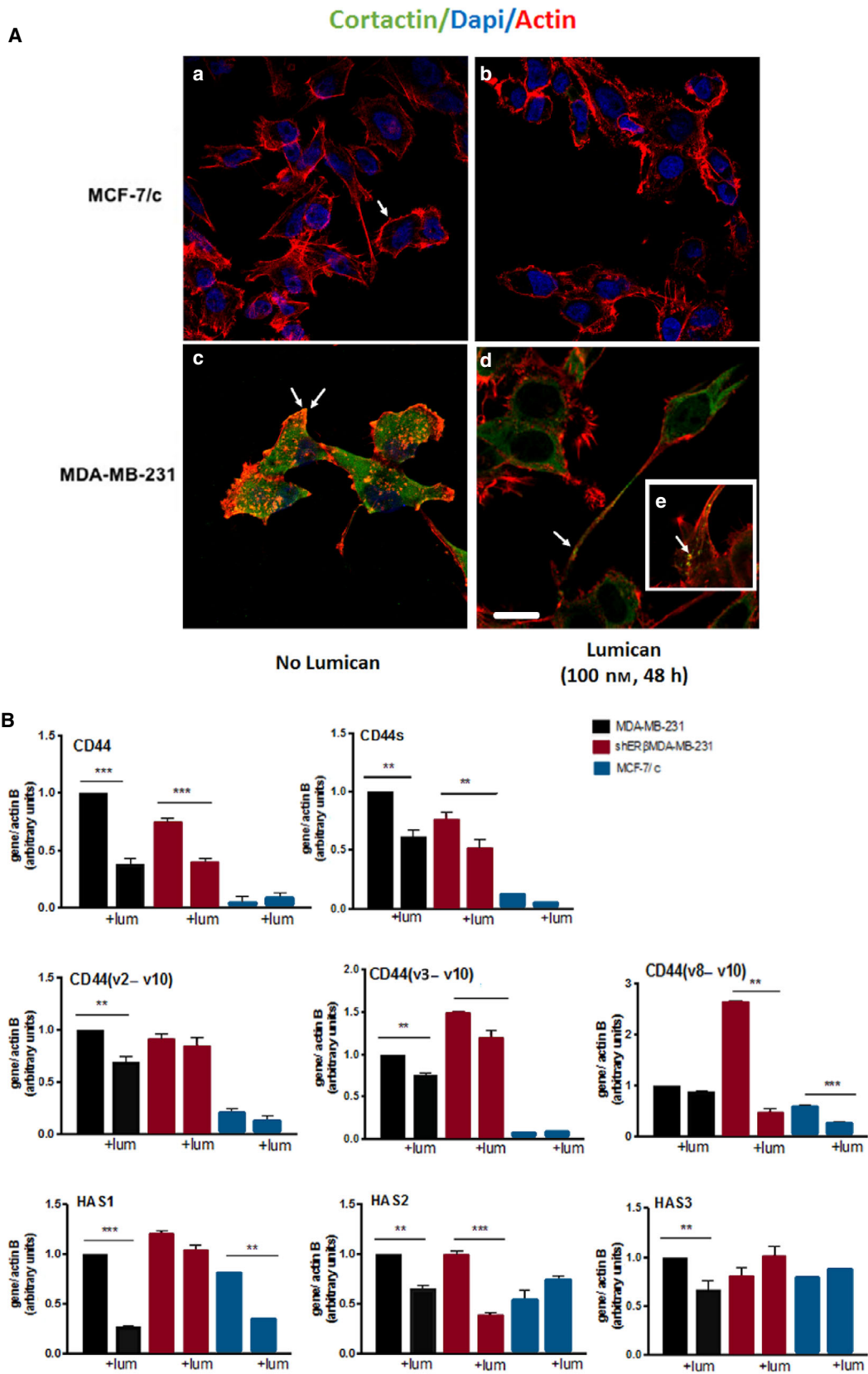


Fig. 2. Lumican is an inhibitory effector of invadopodia marker expression in breast cancer. (A) Confocal immunofluorescence imaging of cortactin in MCF-7/c and MDA-MB-231 cells. In low-invasive MCF-7/c cells, cortactin labeling was detected all along the membrane of cohesive MCF-7/c cells (a), whereas after lumican (100 nM) treatment, the expression of cortactin was drastically decreased (b). A slight actin cytoskeleton re-arrangement was also observed. Cortactin was abundantly expressed at the cell membrane, the cytoplasm, and the cell–cell contacts of mesenchymal MDA-MB-231 cells (c). The presence of 100 nM lumican decreased the expression of cortactin (arrows) in MDA-MB-231 cells (d, e). Scale bar: 10 μ m (a–d). Confocal immunofluorescence experiments were conducted at least in two different experiments (every cell line in triplicate). (B) Effect of lumican on the gene expression levels of CD44, CD44s, CD44 variants (v2–v10, v3–v10, v8–v10), and HA synthases (HAS-1, HAS-2, HAS-3) in breast cancer cell lines. The mRNA expression levels were normalized to beta-actin and quantified using qPCR, as described in the [Materials and methods](#) section. The data shown are representative and taken from 1 out of 3 separate experiments. The major receptor of HA, CD44, was fairly expressed in MCF-7/c cells and decreased in shER β MDA-MB-231 after treatment with 100 nM lumican. However, it was highly expressed in MDA-MB-231 cells, and a significant decrease was noted by the treatment of lumican (ca 62%). The isoform of CD44, CD44s, followed a similar profile, with a significant reduction triggered by lumican (ca 40%) in MDA-MB-231 cells. The effect of 100 nM lumican in CD44 variants was also examined. Lumican affected the v2 variant mostly in MDA-MB-231 cells. It was fairly expressed in the low-invasive MCF-7/c cells and not affected in shER β MDA-MB-231 cells. The v3 variant followed a similar pattern, with the exception of the significant reduction in shER β MDA-MB-231 by lumican (ca 27%). In the case of variant CD44 (v8–v10), paradoxically, 100 nM lumican reduced substantially only its expression in MCF-7/c and shER β MDA-MB-231 cells, revealing that the effect was related to the ER status. The expression of HA synthases was also examined. HAS1 was similarly expressed in all breast cancer cell lines and diminished by the addition of 100 nM lumican. Regarding HAS2, the effect of lumican was most profound in MDA-MB-231 and shER β MDA-MB-231 cells. Regarding HAS3, only MDA-MB-231 cells were affected by the treatment of lumican. All samples were analyzed in triplicate, and the results were expressed as mean \pm SD. Statistical significance between groups was calculated with block two-way ANOVA, using the cell line and the presence of lumican as grouping variables, and the post hoc Scheffe's multiple comparisons test and correct analysis. Asterisks (*), (**), and (***) indicate statistically significant differences ($P < 0.05$, $P < 0.01$, and $P < 0.001$, respectively).

of invadopodia and suggested that lumican inhibited the invadopodia formation. As expected, in the low-invasive and low-metastatic MCF-7/c cells, the staining of cortactin was very weak, being in agreement with the low-invasive and low-metastatic potential of MCF-7/c cells.

In the presence of lumican, staining of cortactin was even weaker, confirming the anticancer effect of lumican even in a low-invasive cell line.

Lumican alters the expression of CD44, its isoform and variants, and hyaluronan synthases in breast cancer cell lines

The content of hyaluronic acid is low in normal breast tissue, but in 56% of breast cancer cases, high levels of HA are found in malignant epithelium and peritumoral stroma [42,43]. Taking into account that the increased HA accumulation, especially in the tumor stroma, signals the metastatic dissemination of cancer, as well as the poor prognosis, the effect of the major receptor of HA, CD44, its isoform and its variants, and the synthases of HA was investigated in breast cancer cell lines of different estrogen receptor status.

As reported, a high HA-rich matrix is related to aggressive tumor behavior, which was also confirmed by the high expression of CD44 and all of its variants in MDA-MB-231 cells (Fig. 2B). Moreover, lumican downregulated the expression of all the markers of HA examined, in the highly invasive MDA-MB-231 cells (Fig. 2B).

CD44 was highly expressed in MDA-MB-231 cells and significantly decreased by the treatment of lumican. The expression of CD44 in shER β MDA-MB-231 cells was lower than MDA-MB-231 cells, and it was reduced in the presence of lumican similarly to MDA-MB-231 cells. Low expression of CD44 was observed in MCF-7/c cells, and its expression was slightly increased in the presence of lumican. The isoform of CD44, CD44s, followed a similar profile, but significantly inhibited by lumican in MDA-MB-231 cells. The expression of CD44s was also downregulated in shER β MDA-MB-231 cells, but to a lesser extent, and was even more inhibited by the treatment of lumican. Moreover, the expression of CD44s in MCF-7/c, although faint in comparison with MDA-MB-231, was even more decreased in the presence of lumican. The effect of lumican in the expression of CD44 variants was also examined. Lumican affected the CD44 (v2–v10) variant mostly in MDA-MB-231 cells and not really affected in shER β MDA-MB-231 cells. CD44 (v2–v10) was poorly expressed in the low-invasive MCF-7/c cells. The CD44 (v3–v10) variant followed a similar motif, with the exception of its significant reduction in shER β MDA-MB-231 cells by lumican. On the other hand, the variant CD44 (v8–v10) was highly reduced by lumican in shER β MDA-MB-231 cells, revealing that its effect, at least in the cases of CD44 (v3–v10) and CD44 (v8–v10), was related to the estrogen receptor status.

The expression of HA synthases was also examined (Fig. 2B). HAS1 was about similarly expressed in all

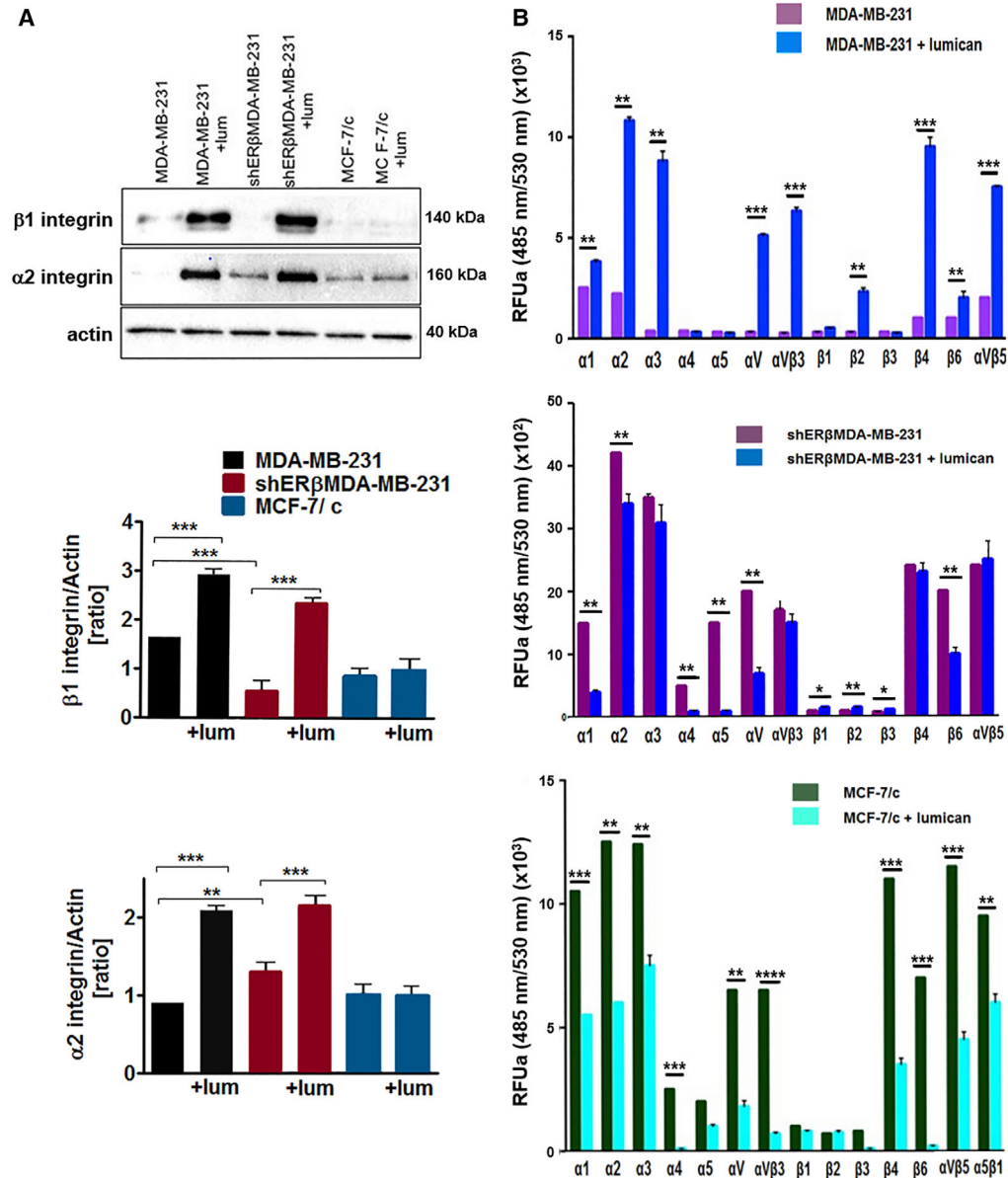


Fig. 3. Lumican effect on RGD/collagen-binding and cell surface integrins according to the ER status of breast cancer cells. (A) Lumican effect on $\alpha 2$ and $\beta 1$ integrin protein expression in breast cancer cell lines. Western immunoblots for $\alpha 2$ and $\beta 1$ integrins and actin for normalizing purposes in MDA-MB-231, shER β MDA-MB-231, and MCF-7/c breast cancer cells before and after treatment with 100 nm lumican for 48 h. (B) Lumican affects the adhesion of breast cancer cells to integrin subunits. First panel: Evaluation of MDA-MB-231 cell adhesion to substrates coated with integrin-specific antibodies. Treatment with 100 nm lumican markedly increased adhesion to all substrates. Second panel: Evaluation of shER β MDA-MB-231 cell adhesion to substrates coated with integrin-specific antibodies. In the presence of lumican, the adhesion of most substrates, especially of α subunits, was markedly reduced. All measurements of the integrin adhesion are normalized to the controls. Third panel: Evaluation of MCF-7/c cell adhesion to substrates coated with integrin-specific antibodies both in the absence and in the presence of 100 nm lumican. Treatment of MCF-7/c cells with lumican significantly downregulated adhesion to all substrates. All samples were analyzed in triplicate, and the results were expressed as mean \pm SD. Statistical significance between groups was calculated with block two-way ANOVA, using the cell line and the presence of lumican as grouping variables, and the post hoc Scheffe's multiple comparisons test and correct analysis. Statistically significant differences are shown as * $P < 0.05$, ** $P < 0.01$, and *** $P < 0.001$.

breast cancer cell lines, and its expression was reduced by lumican. The reduction was higher in MDA-MB-231 cells (about 75%) and less in shER β MDA-MB-231 cells (about 20%). Regarding HAS2, the reducing effect of lumican was more profound in MDA-MB-231 and especially in shER β MDA-MB-231 cells (about 65%), whereas in MCF-7/c cells, a slight increase, but of no statistical significance, of its expression was observed. Regarding HAS3, its expression was reduced in only MDA-MB-231 cells by the treatment of lumican.

Lumican upregulates the $\alpha 2$ and $\beta 1$ integrin expression in MDA-MB-231 and shER β MDA-MB-231, in comparison with MCF-7/c breast cancer cells

The protein expression of the collagen-binding monomer integrins $\alpha 2$ and $\beta 1$ was investigated by western blot in MDA-MB-231, MCF-7/c, and shER β MDA-MB-231 breast cancer cells (Fig. 3A).

The $\alpha 2$ integrin subunit was poorly expressed in almost all cell lines, especially in the most invasive MDA-MB-231. In contrast, after treatment with 100 nm lumican for 48 h, $\alpha 2$ integrin expression was upregulated almost twice in MDA-MB-231 and shER β MDA-MB-231 cells. The poor expression of the $\alpha 2$ and $\beta 1$ monomer integrins was observed in breast cancer cell lines, but its expression was upregulated in the presence of lumican in MDA-MB-231 and shER β MDA-MB-231 cells (Fig. 3A). It is quite noticing that integrin subunit expression was almost not affected in MCF-7/c cells by lumican.

Lumican affects the adhesion of breast cancer cells to integrin subunits

The effect of lumican on cell adhesion was investigated by analyzing the profile of alpha and beta integrins involved in breast cancer cell adhesion in the absence or presence of lumican. After 48-h incubation with lumican (100 nm), laminin- and collagen-binding integrin-mediated cell adhesion was significantly upregulated in the highly invasive MDA-MB-231 cell line. Specifically, $\alpha 1$, $\alpha 2$, $\alpha 3$, αV , $\alpha V\beta 3$, $\beta 2$, $\beta 4$, $\beta 6$, and $\alpha V\beta 5$ were significantly upregulated by lumican (Fig. 3B). Concerning the shER β MDA-MB-231 cell line, $\alpha 1$, $\alpha 2$, $\alpha 4$, $\alpha 5$, αV , and $\beta 6$ integrins were downregulated by lumican, while $\beta 1$, $\beta 2$, and $\beta 3$ were upregulated suggesting a critical role of ER β in the expression levels of adhesive molecules (Fig. 3B). On the other hand, regarding the low-invasive MCF-7/c cells, the protein array of integrin expression demonstrated that lumican downregulated the cell surface and 'RGD-binding' heterodimers $\alpha 5\beta 1$, $\alpha V\beta 5$, and

$\alpha V\beta 3$. Moreover, the monomers $\alpha 1$, $\alpha 2$, $\alpha 3$, $\alpha 4$, αV , $\beta 4$, and $\beta 6$ were significantly downregulated by 48-h treatment with 100 nm lumican (Fig. 3B). Therefore, lumican promoted downregulation of important adhesion elements. Conclusively, in low-invasive MCF-7/c cells, lumican exerted suppressive effects in collagen-binding ($\alpha 1$, $\alpha 2$, $\beta 1$), laminin-binding ($\alpha 3$, $\beta 4$), and fibronectin-binding integrins ($\alpha 5$, αV , $\beta 1$, $\beta 6$, $\alpha V\beta 5$, $\alpha 5\beta 1$). The effect was similar in suppressed ER β MDA-MB-231 cells. On the other hand, in the highly invasive MDA-MB-231 cells, collagen-, fibronectin-, and laminin-binding integrins were upregulated by lumican. All these findings were in accordance with our observations that the adhesion of cells in collagen was increased in the presence of lumican.

Lumican inhibits FAK phosphorylation of tyrosine 397

The inhibition of breast cancer cell migration by lumican is closely related to the inhibition of the phosphorylation of focal adhesion kinase (FAK). FAK phosphorylation status was studied by western blot in MDA-MB-231 control cells (Fig. 4A). Cells were cultured in the absence and presence of lumican for 0, 5, 10, and 15 min. The kinetic of phosphorylation of FAK at tyrosine 397 showed that the level of phosphorylation was relatively low at 0 min and slightly altered by the addition of lumican. The phosphorylation at tyrosine 397 was increased at 5 min, but not altered by the presence of lumican. At 10 min, the phosphorylation was significantly increased in the absence of lumican, but was significantly decreased (by approximately 25%) in the presence of lumican. A peak was noted at 15 min, showing an increase of phosphorylation by 85% in the absence of lumican, while it was reduced by 40% after incubation with lumican. Specifically, after 15 min of incubation of MDA-MB-231 cells with lumican, the FAK-pY397/total FAK ratio was decreased by 40% in comparison with the FAK-pY397/total FAK ratio in the absence of lumican. This result suggested that lumican may also inhibit breast cancer cell migration by inhibiting FAK phosphorylation at tyrosine 397. The kinetic of phosphorylation has been conducted in three different experiments. Focal adhesions signal the biochemical and mechanical characteristics of the ECM and are responsible for the information transport toward the cell. FAK is a nontyrosine kinase with a governing role in cell migration, since it regulates the formation of lamellipodia and transmits the signals between integrins and growth factors. With regard to integrin or growth factor stimulation, FAK is phosphorylated at

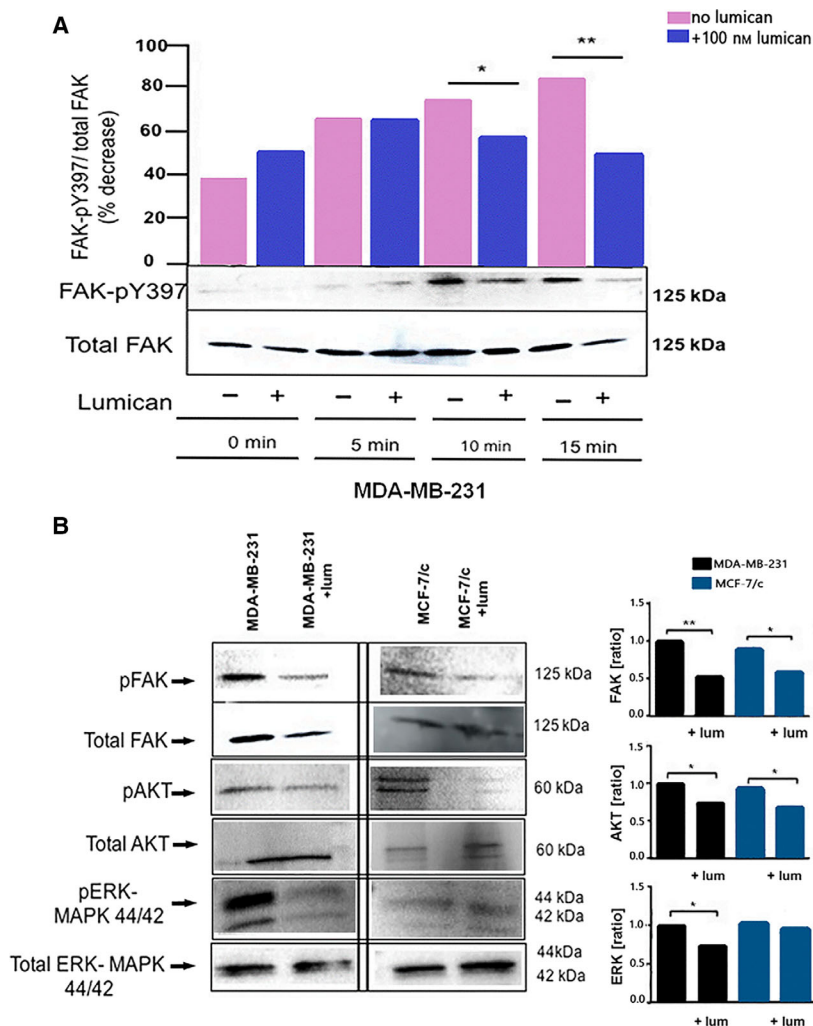


Fig. 4. Lumican decreases the phosphorylation of specific kinases involved in signal transduction. (A) FAK phosphorylation at tyrosine 397 in MDA-MB-231 cells in the absence and presence of 100 nM lumican. Focal adhesion phosphorylation in MDA-MB-231 cells before and after incubation of the cells for 0, 5, 10, and 15 min with 100 nM lumican was analyzed by western blot with antibodies against phosphorylated FAK (pY397) and normalized with anti-total FAK. (B) Lumican decreased the phosphorylation of specific kinases involved in signal transduction before and after treatment with 100 nM lumican for 15 min. After densitometric analysis of the intensity of the bands, the resulting ratio of phosphorylated form to total kinase protein intensity was calculated and presented in the graph. Statistical significance between groups was calculated using Student's *t*-test. Data are presented as mean values \pm SD from three independent experiments (* $P < 0.05$; ** $P < 0.01$).

Tyr-397, which eventually facilitates the binding of Src kinases, the p85 regulatory subunit of PI3K, and phospholipase C. FAK is also implicated in the signaling of several other pathways. As an example, a complex of Akt-Src can affect the phosphorylation of components, which are implicated in cell adhesion and cell migration. Consequently, the phosphorylation of several mediators in cell signaling was also examined following the same peak of phosphorylation at 15 min, as FAK.

The phosphorylation of specific proteins implicated in signal transduction in control MDA-MB-231 and MCF-7/c cells incubated 15 min with 100 nM lumican was analyzed by western blot. Altered phosphorylation was noticed regarding most of the proteins, when the cells were cultured in the presence of lumican. Lumican reduced the phosphorylation levels of FAK, ERK 1/2 MAPK 42/22, and Akt proteins (Fig. 4B). These results indicate that lumican potentially regulates

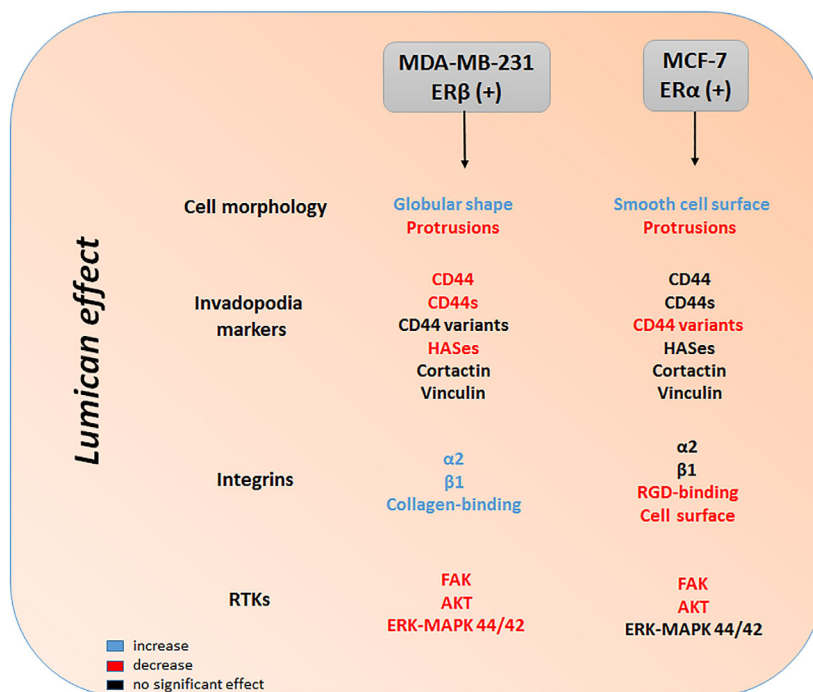
RTKs and affects their downstream mediators. The results of the present report are summed up in Fig. 5.

Discussion

The effects of lumican on the regulation of ERs-associated functional properties of breast cancer cells, expression of matrix effectors, and EMT were recently addressed. However, the molecular mechanisms which might be responsible for the anticancer activity of lumican in invasive breast cancer are still not described in the literature. Thus, the aim of this study was to investigate a series of molecules to unravel mechanisms that could be related to the recorded functional effects of lumican.

Concerning lumican effect on cell morphology, both MDA-MB-231 and MCF-7/c cells after 24 and 48 h of culture seemed to favor cell grouping and cell-cell contact. The development of invadopodia and cytoplasmic protrusions was reduced, as well as the formation of

Fig. 5. Diagram summarizing the major effects of lumican in breast cancer cells. The actions of lumican have been classified according to its effect on cell morphology (cell surface of breast cancer cells and protrusions of migrating cells), invadopodia markers (HA molecules, i.e., CD44, CD44s, HASes, as well as cortactin), integrins (collagen/laminin/RGD-binding integrins and cell surface integrins), and RTKs (FAK, Akt, ERK-MAPK 44/42), according to the expression of estrogen receptors alpha and beta.



microvesicles and microvilli on cell surface, which are highly related to cancer cell aggressiveness. This last effect was particularly evident in MCF-7/c cells, whose shape was resembling billiard balls, with very smooth cytoplasmic surface completely avoid of extravesicles.

The expression of several matrix molecules, such as HA synthases, CD44, and invadopodia markers, integrins, and signaling effectors was analyzed. CD44 is upregulated in breast cancer and can be expressed in its standard isoform, CD44s, or as a number of alternatively spliced variant isoforms, CD44v. Multiple CD44 tends to play a role in epithelial phenotype, tumor initiation, and growth and are often associated with metastatic lesions. More specifically, CD44 (v2–v10), CD44 (v3–v10), and CD44(v8–v10) were investigated in this study, as CD44 (v2–v10) is used as a clinical prognostic marker for pancreatic ductal adenocarcinoma (PDAC), as well as breast cancer, since this variant is associated with the positive ER and PgR status, low S-phase fraction, and postmenopausal age [44]. CD44 (v3–v10) is implicated in cell migration, cell proliferation, and cisplatin resistance, and is also associated with positive steroid receptor status and negative/low HER2 status [44,45]. The variant CD44 (v8–v10) is responsible for the tumor initiation in gastric cancer and is also found to be overexpressed in lung and breast cancer [46]. In addition to this, orthotopic injection of CD44 (v8–v10)-expressing breast cancer cells in mice provoked an increase in lung metastasis [47].

In this study, our data suggest that the expression of cortactin, a regulatory marker of invadopodia, and HA-related molecules (CD44, CD44s, CD44-v2, CD44-v3, CD44-v8, HAS-1, HAS-2, HAS-3) was affected by the presence of lumican in regard to the level of expression of ERs. For instance, the expression of CD44 and CD44s was high in MDA-MB-231 cells, moderate in shER β MDA-MB-231, and drastically reduced in the low-metastatic MCF-7/c cells, suggesting an association of CD44 with the ER status. It is also worth noticing that the expression of HAS1 and HAS2, when inhibited in melanoma, which is also a high-metastatic cancer, is related to higher patient survival, faster recuperation, and less possibilities for metastasis [48]. Treatment with lumican of breast cancer cells indicated a lower expression of the HA synthases. It is worth noticing that increased expression of HAS2 or HAS3 renders them as key regulators of EMT and associates them with enhanced cell growth, migration, and invasion [49]. In our study, statistically significant data demonstrated that the HA synthases were inhibited by the presence of lumican, being in agreement with the lumican anticancer effect. These data are also supported by SEM analysis, which showed that lumican treatment reduces the presence of extravesicle production, which are described to be a major site of expression of HA by in cancer cells [50].

Collectively, these results rendered the role of lumican crucial and lead us to further investigate the

regulation of HA metabolism, as it could constitute a future target for a therapeutic standpoint.

Several cell surface receptors of lumican were characterized and described [35]. Cell adhesion is a fundamental cell function, as it regulates the development and maintenance of tissues. Integrins, a family of cell surface receptors, mediate cell attachment to proteins of the ECM. They are heterodimer molecules, comprising of an alpha and beta transmembrane glycoprotein subunit, noncovalently bound to each other. Since lumican regulates cell adhesion and migration of melanoma cells by altering the actin network and focal adhesion through $\alpha 2\beta 1$ integrin, a cell adhesion assay involving integrins was performed [51–53]. It was found that lumican increased cell adhesion by $\alpha 1$, $\alpha 2$, $\alpha 3$, αV , $\beta 4$, $\beta 6$, $\alpha V\beta 3$, and $\alpha V\beta 5$ integrins in MDA-MB-231 cells, while decreasing MCF-7/c cell adhesion mediated by these integrins.

$\alpha 2\beta 1$ integrin is reported to be decreased in cancer cells, probably because of enhanced tumor cell dissemination levels. It was shown that when $\alpha 2\beta 1$ is re-expressed in breast cancer, many cancer cell functions are reversed, endowing $\alpha 2\beta 1$ as a molecule with tumor suppressive properties [54,55]. This hypothesis seems to be confirmed by the weak expression of the $\alpha 2$ and $\beta 1$ monomer integrins in the breast cancer cell lines, as well as their enhanced expression in the presence of the antitumorigenic lumican. In this study, lumican was shown to increase the expression of $\alpha 2$ and $\beta 1$ integrin subunits in the metastatic MDA-MB-231 cells, as well as in shER β MDA-MB-231 as compared to the low-invasive MCF-7/c. Integrins $\alpha 3\beta 1$, $\alpha 6\beta 1$, $\alpha 6\beta 4$, and $\alpha 7\beta 1$ comprise the laminin-binding cell adhesion receptors. Integrin $\alpha 3\beta 1$ might be one of the receptors for laminin in the presence of lumican since subunit expression was increased in the presence of lumican in MDA-MB-231 cells and the adhesion of MDA-MB-231 cells on $\alpha 3\beta 1$ was increased in our adhesion assay in the presence of lumican. Most probably, $\alpha 6\beta 1$ or $\alpha 6\beta 4$ is excluded of being laminin-binding integrins, since $\alpha 6$ adhesion was very low in our study, and consequently, $\beta 1$ and $\beta 4$ would be without partner.

The effect of $\alpha 3\beta 1$ is reported to be contradictory. For example, in breast carcinoma, both positive and negative correlation has been reported. *In vitro* experiments showed that when $\alpha 3\beta 1$ integrin is blocked, cancer cells seem to lose their tendency to adhere, invade, and metastasize at distant sites. Moreover, when cell–substrate adhesion is mediated by $\alpha 3\beta 1$, cancer cells are not easily detached from the primary tumor site, in order to metastasize [56]. Moreover, there are several studies describing $\alpha 3\beta 1$ as negative regulator of cell migration. For example, *in vitro* study proved that $\alpha 3$ -

knockout keratinocytes presented increased cell motility *in vitro* and faster wound healing *in vivo* [57]. The antimigratory capacity of $\alpha 3\beta 1$ is accompanied by the ability to promote stable cell–cell junctions. It was recently demonstrated that $\alpha 3\beta 1$ integrin localizes to cell–cell junctions in keratinocytes, and cell adhesion can be blocked, when $\alpha 3\beta 1$ is inhibited [58]. Therefore, the decreased scattering on laminin is associated with a decreased number of actin fibers, as well as the focal adhesions on integrin ligand sites [59].

It is worth noticing that $\alpha 7$ subunit was not analyzed in our study, since in comparison with $\alpha 3$ and $\alpha 6$ integrin subunits, relatively little is known about the role of a $\alpha 7\beta 1$ integrin in tumorigenesis. $\alpha 7$ integrin has a potential tumor suppressive role in several cell types, probably because of upregulation of the inhibitors of cyclin-dependent kinases and Rac family small GTPases [60]. Therefore, $\alpha 7$ subunit could comprise a perspective of this study, in order to investigate whether this subunit is also involved as laminin receptor in the presence of lumican.

The binding of integrins to focal adhesions transmits signals from the extracellular environment to the intracellular network, and inversely. This transmission is mediated by integrins and downstream signaling pathways, such as FAK, ERK 1/2 MAPK 42/44, and Akt, which were downregulated by lumican. Moreover, the dimers $\alpha V\beta 5$ and $\alpha 2\beta 1$ are associated with tumor development, as they mediate epithelial cell adhesion to the basement membrane as well as they promote cancer cell migration, proliferation, and survival. Moreover, in adult epithelia, $\alpha 5\beta 1$ is fairly expressed, but in case of cancer, its expression is enhanced [39,61–63].

From all the above, it could be concluded that lumican seemed to have more profound effect on the most aggressive cells examined, MDA-MB-231 cells, but also on shER β MDA-MB-231 cells, which possess an epithelial-like phenotype. Upregulation of CD44, its isoform and its variants, as well as of HA synthases, correlates with EMT and breast cancer metastasis and lumican downregulated them, in accordance with its anticancer activity. Breast cancer metastasis, resulted in part from increased capacity for cancer cell intravasation, is also influenced by downregulation of $\alpha 2\beta 1$ integrin, and lumican was reversing their expression in both MDA-MB-231 and shER β MDA-MB-231 cells. In addition, cell adhesion is lowering in cancer, and considering cell adhesion mediated by integrins, lumican increased cell adhesion in MDA-MB-231 cells and had no substantial effect on shER β MDA-MB-231 cells. These observations, taken together, render critical the synergism of lumican and ER β and may lead to further investigate as a target for a therapeutic start point.

Furthermore, several reports demonstrated that lumican acts by downregulating phosphorylation of major cellular kinases of cell migration and proliferation/survival signaling, like ERK, Akt, FAK, and mTOR [39,64–68]. However, still most of the mechanisms remain unidentified. There is a plethora of data about decorin, which inhibits Met receptor signaling and specifically leads to a noncanonical repression of beta-catenin and Myc4 [69]. Collecting the data from this study, our hypothesis is that lumican interacts through integrins and inhibits FAK phosphorylation, which leads to the downregulated phosphorylation of ERK and Akt. Moreover, the inhibition of breast cancer cell migration by lumican is closely related to the inhibition of the phosphorylation of FAK.

The downregulated phosphorylation of ERK and the reduction of the downstream signaling events result in decrease of lamellipodia formation and MMP-14 activity, leading to an inhibition of cell migration. Moreover, the inhibition of PI3-Akt kinase results in a decrease of its activity and to a reduction of the downstream signaling cascade, which may induce inhibition of cell growth.

It was recently published that the suppression of ER β in the highly invasive MDA-MB-231 breast cancer cells, which rendered an inhibition of EMT, triggered pivotal alterations in the gene and protein expression levels of ECM key components, like PGs, which, respectively, led to altered behavior of breast cancer cells [70]. miRNAs are governors of the metastasis and promotion of cancer, and they may serve as novel targets for therapeutic approaches of breast cancer [71,72]. Unpublished data of our research group showed that there is a possible synergistic effect of miRNAs with the anticancer effect of lumican. More specifically, miR let-7d was found to be overexpressed in MDA-MB-231 cells treated with lumican, while overexpression of miR let-7d is reported to reverse the EMT and inhibit the migratory and invasive potential of these cells, confirming the antimigratory properties of lumican. The expression of miRlet-7d was also induced in shER β MDA-MB-231. This effect on miR let-7d may have an impact on the morphology of these cells as miR let-7d is a trigger of EMT, as it increases the expression levels of E-cadherin and N-cadherin, markers of epithelial phenotype, as well as it decreases vimentin, marker of mesenchymal phenotype [73]. Moreover, the gene expression of Mir-200b was found to be significantly induced because of the suppression of ER β , as the members of the 200b family target directly to ER α and ER β [74]. Treatment of MDA-MB-231 and shER β MDA-MB-231 with lumican increased the gene expression of the EMT inhibitor miR-200b, confirming the anticancer effect of lumican. This synergistic effect of lumican with miR-200b may have an effect on the morphology of these

cells, as miR-200b is linked with the mesenchymal phenotype of breast cancer cells, as it is one of the negative regulators of the EMT process, invasion, and metastasis [72,75,76]. Therefore, miRs in synergy with lumican can constitute an innovative therapy targeting inhibition of oncogenic signaling and breast cancer progression.

In conclusion, the obtained data suggest that the treatment with lumican may be beneficial for breast cancer. Further studies on the mechanisms and specifically on the cell signaling underlying the invadopodia properties, in regard to the ER status, will shed light on cancer metastasis therapy.

Materials and methods

Chemical reagents and antibodies

The culture medium used was the basal medium (Dulbecco's modified Eagle's medium, DMEM), supplemented with 10% FBS, 1.0 mM sodium pyruvate, 2 mM L-glutamine, and a cocktail of antibiotics (100 IU·mL⁻¹ penicillin, 100 μ g·mL⁻¹ streptomycin, 10 μ g·mL⁻¹ gentamycin sulfate, and 2.5 μ g·mL⁻¹ amphotericin B). DMEM, FBS, sodium pyruvate, L-glutamine, penicillin, streptomycin, amphotericin B, and gentamycin were all obtained from Biosera LTD (Courtaboeuf Cedex, France).

Cell culture

Breast cancer, low-metastatic and ER α -positive MCF-7/c cells (#HTB-22TM), and highly metastatic, ER β -positive MDA-MB-231 cells (#HTB-26TM) were obtained from ATCC^R. The control cells were cultured in standard conditions of humidified 95% air/5% CO₂ incubator at 37 °C. MDA-MB-231 cells were transfected with shRNA against human ER β or nontargeting shRNA control using polybrene solution (sc-134220; Santa Cruz Biotechnology, Inc, Heidelberg, Germany) according to the manufacturer's instructions as previously described [2,3]. In order to establish the stable clones, culture medium was supplemented with 0.8 μ g·mL⁻¹ puromycin dihydrochloride (sc-108,071; Santa Cruz Biotechnology, Inc). In all experiments, cell viability was verified and measured higher than 95% by trypan blue exclusion test. When necessary, lumican (2846-LU; R&D systems, Minneapolis, MN, USA) was added in the cell culture medium at the concentration of 100 nM and cells were incubated during 24 or 48 h according to the type of assays.

Cell adhesion

?A3B2 t1sb = -.015w? > Cell adhesion was performed with the CHEMICON[®] Alpha/Beta Integrin-Mediated Cell Adhesion Array Combo Kit (Fluorimetric-ECM535; Sigma-Aldrich Chemie, Saint-Quentin Fallavier, France). The kit principle

involves the use of mouse monoclonal antibodies generated against human alpha ($\alpha 1$, $\alpha 2$, $\alpha 3$, $\alpha 4$, $\alpha 5$, and αV), beta ($\beta 1$, $\beta 2$, $\beta 3$, $\beta 4$, and $\beta 6$) integrin subunits, and $\alpha V\beta 3$, $\alpha V\beta 5$, and $\alpha 5\beta 1$ integrins, which are immobilized onto a goat anti-mouse antibody-coated microtiter plate. Cells expressing these integrins on their cell surface are captured in the plate. Afterward, unbound cells are removed, and the adherent cells were lysed and detected by the patented CyQuant GR dye (Thermo Fisher Scientific, Illkirch, France). This green-fluorescent dye exhibits strong fluorescence enhancement when bound to cellular nucleic acids. Relative cell attachment was determined using a fluorescence plate reader. Specifically, cells were seeded up to 80% confluence. Using the nonenzymatic dissociation buffer (PBS/2–5 mM EDTA) for 20 min, cell suspensions were prepared. Cell suspensions from every cell line, using Hank's buffered salt solution with 0.1% BSA, 25 mM HEPES, and 1 mM $\text{Ca}^{2+}/\text{Mg}^{2+}$, were prepared of a cell density of 2.0×10^6 cells·mL⁻¹. Hundred microlitre of each cell suspension was added to each well of the mouse anti-alpha or anti-beta integrin and negative control captures, in triplicate for every sample.

After seeding the cells, the plates were incubated for 1–2 h at 37 °C in a CO₂ incubator. Cell culture media were removed, cells were hydrated with assay buffer, and plates were incubated for 15 min in the CO₂ incubator. A solution of 150 μL from every well was transferred to a new plate suitable for fluorescence measurement. Fluorescence was finally measured by a fluorescence plate reader using 485 excitation/530 nm emission filters.

3D cell invasion assay

The invasive behavior of breast cancer cells was assessed by using the Boyden chamber assay according to the method of Albini [77–79]. Negative controls were tested as well. Isopore membrane filters (Millipore®) with pore size of 8.0 μm were used for the assays. Filters were coated with 50 μL of 50 $\mu\text{g}\cdot\text{mL}^{-1}$ collagen type I as previously described [41]. For every cell line, 2×10^5 cancer cells·mL⁻¹, previously resuspended in 800 μL serum-free medium, were seeded on top of the polymerized gel in the upper chamber. Cells were seeded on collagen type I-coated filters in the absence or in the presence of 100 nm lumican in the cell culture medium for 24 or 48 h at 37 °C. Conditioned media were used as chemoattractant, added in the lower chamber. Millipore filters were removed 24 or 48 h of incubation at 37 °C. The filters were washed with PBS, fixed in 100% ethanol for 5 min, and stained with 1% toluidine blue/1% sodium tetraborate for 2 min.

Scanning electron microscopy

MDA-MB-231 and MCF-7 breast cancer cells were seeded on sixteen 'Isopore membrane filter' with pore size of 8.0 μm (Millipore) coated by type I collagen (50 μL of 50 $\mu\text{g}\cdot\text{mL}^{-1}$) with the addition of 100 nm lumican as previously described [41] for 3D collagen cultures. Similarly,

MCF-7 and MDA-MB-231 breast cancer cells were seeded in eight similar 3D collagen cultures with no addition of lumican in order to be used as control groups. After 24 and 48 h, Millipore filters with adhering cells were fixed in a Karnovsky's solution for 20 min, rinsed three times with 0.1% cacodylate buffer, dehydrated with increasing concentrations of ethanol, and finally dehydrated with hexamethyldisilazane (Sigma-Aldrich Inc.) for 15 min. Millipore filters were then mounted on proper stubs and coated with a 5-nm palladium-gold film (Emitech 550 sputter coater, Kolzer, SRL, Milan, Italy) to be observed under a scanning electron microscope (SEM) (Philips 515, Eindhoven, the Netherlands) operating in secondary electron mode.

Laser scanning microscopy

For immunofluorescence/confocal microscopy experiments, cells were seeded on sterile glass coverslips in 24-well plates and grown to 50% confluence before treatment. MDA-MB-231 and shER β MDA-MB-231 cells were seeded at 5×10^5 cells/well. MCF-7/c cells were seeded at 10×10^5 cells/well. Cells were rinsed twice in PBS, fixed using 4% paraformaldehyde (in PBS buffer) pH 7.2 for 15 min at room temperature, and washed three times with PBS-Tween buffer. After saturation with 3% BSA for 30 min at room temperature, cells were incubated overnight at 4 °C with the appropriate primary antibody (Table 1). The dilutions for the primary antibodies, used for the detection of each protein, are displayed in Table 1. For the detection of actin cytoskeleton, cells were permeabilized with 0.1% Triton X-100 and incubated 1 h at room temperature with Alexa Fluor® 568-conjugated phalloidin at 1/200 dilution. Negative controls were also prepared after staining with mouse IgG, isotype control. Slides were observed under confocal laser scanning microscope (Zeiss LSM 700, Zeiss, Paris, France).

RNA isolation and real-time PCR analysis

Total RNA of breast cancer cells was isolated using RNeasy Plus Mini Kit (Qiagen, Courtaboeuf, France) according to the instructions of the manufacturer. RNA quality was examined and determined on an Agilent 2100 Bioanalyzer (Agilent Technologies, Massy, France). Afterward, reverse transcription was performed at 50 °C for 30 min using the Maxima First Strand™ cDNA Synthesis Kit (Thermo Scientific, Villebon and Yvette, France) with 1 μg of total RNA. The ABI PRISM Instrument (Thermo Fisher Scientific) was used for the experiments, and the specific primers for each gene were purchased from Thermo Fisher Scientific. All primer sequences and sizes of the PCR product of each targeted gene are presented in Table 2. The specificity of PCR amplification products was assessed by dissociation-melting curve analysis. After the reaction was completed, C_t value was calculated from the

Table 1. List of primary antibodies used in western blot (WB) and immunocytochemistry (ICC) experiments.

Recognized protein	Host and isotype	Dilution	Reference
Actin	Polyclonal goat IgG	WB: 1/1000	Sc-1616; Santa Cruz Biotechnology
Akt	Monoclonal rabbit IgG	WB: 1/1000	4691; Cell Signaling Technology (Leiden, the Netherlands)
Cortactin p80/p85 (clone 4F11)	Monoclonal mouse IgG1	WB: 1/2000 ICC: 1/100	05-180; Millipore®
ERK 1/2 MAPK 42/44	Rabbit IgG1	WB: 1/1000	9102; Cell Signaling Technology
FAK	Polyclonal Rabbit IgG	WB: 1/1000	Sc-932; Santa Cruz Biotechnology
GSK3 α/β	Monoclonal rabbit IgG	WB: 1/1000	5676; Cell Signaling Technology
Integrin α 2-cd49b	Monoclonal Mouse IgG2 α	ICC: 1/100	611016; BD Biosciences (Claix, France)
Integrin α 2 (blocking)	Monoclonal Mouse IgG1	WB: 1/1000	MAB1950; Millipore®
Integrin β 1-cd29b	Mouse IgG1	ICC: 1/100	610467; BD Biosciences
Integrin β 1	Polyclonal rabbit IgG	WB: 1/1000	AB1952P; Millipore®
P130Cas	Monoclonal Mouse IgG1	WB: 1/1000	610271; BD Transduction Laboratories™ Null, US
Phospho-Akt (ser473)	Monoclonal rabbit IgG	WB: 1/1000	4060; Cell Signaling Technology
Phospho-ERK 1/2 MAPK 42/44	Rabbit IgG	WB: 1/1000	4370; Cell Signaling Technology
Phospho-FAK	Monoclonal Mouse IgG	WB: 1/300	05-1140; Millipore®
Phospho-GSK3 α/β	Monoclonal rabbit IgG	WB: 1/1000	9323; Cell Signaling Technology
Phospho-p130Cas (Tyr410)	Polyclonal rabbit IgG	WB: 1/1000	4011; Cell Signaling Technology

Table 2. List of primers used for real-time PCR.

Gene	Amplicon size (bp)	Accession number
CD44	70	Hs01075861_m1 Thermo Fisher Scientific
CD44s	108	Hs01081473_m1 Thermo Fisher Scientific
CD44 (v2–v10)	66	Hs01075866_m1 Thermo Fisher Scientific
CD44 (v3–v10)	63	Hs01081480_m1 Thermo Fisher Scientific
CD44 (v8–v10)	82	Hs01081475_m1 Thermo Fisher Scientific
HAS1	105	Hs00155410_m1 Thermo Fisher Scientific
HAS2	63	Hs00193435_m1 Thermo Fisher Scientific
HAS3	60	Hs00193436_m1 Thermo Fisher Scientific
β Actin	171	Hs99999903_m1 Thermo Fisher Scientific

amplification plots. Each sample was normalized to the housekeeping gene transcript gene (β -Actin). The results of relative quantifications were obtained with the use of the $\Delta\Delta C_t$ method. PCR assays were conducted at least three times in triplicates for each sample.

Western blot analysis

Total cell proteins were prepared from cell monolayers after being washed twice with PBS and detached after scrapping in cell lysis buffer (50 mM Tris/HCl, pH 7.6, 0.5 M NaCl, 0.02%

NaN₃, 0.6% NP40, 5 mM EDTA, 1 mM iodoacetamide, 1 mM PMSF, 1 mM Na₃VO₄, and Protease Inhibitor Cocktail) (Sigma-Aldrich Chemi). The Bradford method was used for measuring the protein concentration.

Total cell proteins (30 μ g) were mixed with 5 \times Laemmli buffer (1.25 M Tris, 10% SDS, 20% sucrose, pH 6.8, 0.005% bromophenol blue) and β -mercaptoethanol, to obtain a final concentration of the latter of 3%. The total volume of the samples is maximum of 30 μ L, with the precondition that all the loading samples have the same concentration. Samples were denatured for 5 min at 95 °C and were then subjected to electrophoresis in a polyacrylamide gel (concentration range: 7.5–15%, containing 0.1% SDS). Proteins were transferred by electroblotting onto Hybond-P PVDF membranes (GE Healthcare, Orsay, France), previously activated for 10 s in methanol. The membranes were saturated in TBS-T solution (0.1% Tween-20, 20 mM Tris, and 140 mM NaCl, pH 7.6) containing 5% nonfat milk (Bio-Rad, Marnes-la-Coquette, France) or 5% BSA for 2 h at room temperature. Membranes were incubated overnight at 4 °C with constant gentle shaking with primary antibodies (Table 1). The next day, membranes were washed three times with TBS-T and incubated with a 1 : 10 000 dilution of the adequate corresponding secondary antibody conjugated to horseradish peroxidase in 1% nonfat milk or 1% BSA, in TBS-T for 1 h at room temperature. After three washes with TBS-T, the bands were visualized by the ECL Prime Chemiluminescence Detection reagent (GE Healthcare), according to the manufacturer's instructions. The chemiluminescence signal was captured using a ChemiDoc™ MP Imaging (Bio-Rad).

Phosphorylation analysis

Western blot experiments concerning the signaling pathways require a specific way of preparation of the cell

lysates. For every cell line, 5×10^6 cells were required as a starting point. Cells were rinsed twice with a buffer containing 50 mM HEPES, 126 mM NaCl, 5 mM KCl, and 1 mM Na₂EDTA. Then, cells were incubated for 5 min at 37 °C to detach in the above buffer. Serum-free basal medium was added, and the cell suspensions were centrifuged for 1 min at 400 *g* at 4 °C. The cell pellets were resuspended in serum-free basal medium and separated in low-binding tubes (in order to avoid lower protein absorbance).

Every tube corresponds to a time point: 0, 5, 10, 15 min. Cell suspensions were prepared both in the absence and presence of lumican (100 nM), which was added at 0-min time point. All samples were placed in a carousel at 37 °C and were pulled according to the time point. All the gathered samples (final volume 100 µL) were placed on ice and then centrifuged at 400 *g* at 4 °C. Pellets were resuspended in lysis buffer (2% SDS in 50 mM Tris, pH 7.4, 150 mM NaCl, 5 mM EDTA, 10 mM NaF, 2 mM Na₃VO₄, 1 mM PMSF, 10 µg·mL⁻¹ leupeptin, 10 µg·mL⁻¹ aprotinin). Samples were centrifuged at 1400 *g* at 4 °C for 15 min. Supernatants were collected, and their protein concentration was measured by the Bradford assay. Proteins were denatured at 95 °C for 5 min before western blot. The experiments were repeated three times.

Statistical analysis

Reported values are expressed as mean ± standard deviation (SD) of experiments in triplicate. Statistically significant differences were evaluated using the analysis of variance (ANOVA) test and were considered statistically significant at the level of at least $P \leq 0.05$. Statistical analysis and graphs were made using GRAPHPAD PRISM 6 (GraphPad Software, San Diego, CA, USA).

Acknowledgements

We wish to thank Pr. F.-X. Maquart and Pr. S. Dukic (University of Reims, Champagne-Ardenne, France) for the technical assistance, suggestions, and useful discussions during the course of this work, and Dr. C. Terryn for the technical support in confocal microscopy. We wish to thank Mr. Gianfranco Filippini DISTAL-Plant Pathology (University of Bologna) for technical assistance during sample preparation for SEM. This research has been cofinanced by the Region Champagne-Ardenne, the Fond Européen de Développement Régional (FEDER), le Contrat de Projet Etat Région CPER 2013–2020, the Ligue contre le cancer, Conférence de Coordination Inter Régionale du Grand Est (CCIR-GE) 30036506-UMR7369, and the PHC Polonium. This publication is part of the joint PhD (University of Patras/University of Reims Champagne-Ardenne) of Konstantina Karamanou, under the financial support of Eiffel Scholarship

of Excellence (870731F), supplied from the French Ministry of Foreign Affairs, as well as General Secretariat for Research and Technology (GSRT) and the Hellenic Foundation for Research and Innovation (HFRI).

Conflict of interest

The authors declare no conflict of interest.

Author contributions

KK performed the main experimental part and prepared the manuscript draft and the figures; MF performed SEM image analysis and SEM results; and MO performed part of 3D collagen invasion assays. AP contributed to the writing of the manuscript and supervised the qPCR experiments. DHV and SB supervised the experiments, demonstration of the data, and contributed to manuscript writing and editing. SB managed the overall supervision and submitted the manuscript. All authors reviewed the manuscript.

References

- Jemal A, Bray F, Center MM, Ferlay J, Ward E & Forman D (2011) Global cancer statistics. *CA Cancer J Clin* **61**, 69–90.
- Bouris P, Skandalis SS, Piperigkou Z, Afratis N, Karamanou K, Aletras AJ, Moustakas A, Theocharis AD & Karamanos NK (2015) Estrogen receptor alpha mediates epithelial to mesenchymal transition, expression of specific matrix effectors and functional properties of breast cancer cells. *Matrix Biol* **43**, 42–60.
- Piperigkou Z, Bouris P, Onisto M, Franchi M, Kletsas D, Theocharis AD & Karamanos NK (2016) Estrogen receptor beta modulates breast cancer cells functional properties, signaling and expression of matrix molecules. *Matrix Biol* **56**, 4–23.
- Allred DC & Swanson PE (2000) Testing for erbB-2 by immunohistochemistry in breast cancer. *Am J Clin Pathol* **113**, 171–175.
- DeSantis C, Siegel R, Bandi P & Jemal A (2011) Breast cancer statistics, 2011. *CA Cancer J Clin* **61**, 409–418.
- Hanstein B, Djahansouzi S, Dall P, Beckmann MW & Bender HG (2004) Insights into the molecular biology of the estrogen receptor define novel therapeutic targets for breast cancer. *Eur J Endocrinol* **150**, 243–255.
- Marotti JD, Collins LC, Hu R & Tamimi RM (2010) Estrogen receptor-beta expression in invasive breast cancer in relation to molecular phenotype: results from the Nurses' Health Study. *Mod Pathol* **23**, 197–204.
- Skloris GP, Lewis A, Emberley E, Peng B, Weebadda WK, Kemp A, Davie JR, Shiu RP, Watson PH & Murphy LC (2007) Estrogen receptor-beta regulates

- psoriasis (S100A7) in human breast cancer. *Breast Cancer Res Treat* **104**, 75–85.
- 9 Fox EM, Davis RJ & Shupnik MA (2008) ERbeta in breast cancer—onlooker, passive player, or active protector? *Steroids* **73**, 1039–1051.
 - 10 Krege JH, Hodgin JB, Couse JF, Enmark E, Warner M, Mahler JF, Sar M, Korach KS, Gustafsson JA & Smithies O (1998) Generation and reproductive phenotypes of mice lacking estrogen receptor beta. *Proc Natl Acad Sci USA* **95**, 15677–15682.
 - 11 Lamouille S, Xu J & Derynck R (2014) Molecular mechanisms of epithelial-mesenchymal transition. *Nat Rev Mol Cell Biol* **15**, 178–196.
 - 12 Hay ED (1995) An overview of epithelio-mesenchymal transformation. *Acta Anat (Basel)* **154**, 8–20.
 - 13 Block MR, Badowski C, Millon-Fremillon A, Bouvard D, Bouin AP, Faurobert E, Gerber-Scokaert D, Planus E & Albiges-Rizo C (2008) Podosome-type adhesions and focal adhesions, so alike yet so different. *Eur J Cell Biol* **87**, 491–506.
 - 14 Revach OY, Weiner A, Rechav K, Sabanay I, Livne A & Geiger B (2015) Mechanical interplay between invadopodia and the nucleus in cultured cancer cells. *Sci Rep* **5**, 9466.
 - 15 Paz H, Pathak N & Yang J (2014) Invading one step at a time: the role of invadopodia in tumor metastasis. *Oncogene* **33**, 4193–4202.
 - 16 Miglarese MR, Mannion-Henderson J, Wu H, Parsons JT & Bender TP (1994) The protein tyrosine kinase substrate cortactin is differentially expressed in murine B lymphoid tumors. *Oncogene* **9**, 1989–1997.
 - 17 Hiura K, Lim SS, Little SP, Lin S & Sato M (1995) Differentiation dependent expression of tensin and cortactin in chicken osteoclasts. *Cell Motil Cytoskeleton* **30**, 272–284.
 - 18 Zhan X, Haudenschild CC, Ni Y, Smith E & Huang C (1997) Upregulation of cortactin expression during the maturation of megakaryocytes. *Blood* **89**, 457–464.
 - 19 Wu H & Montone KT (1998) Cortactin localization in actin-containing adult and fetal tissues. *J Histochem Cytochem* **46**, 1189–1191.
 - 20 Kessels MM, Engqvist-Goldstein AE & Drubin DG (2000) Association of mouse actin-binding protein 1 (mAbp1/SH3P7), an Src kinase target, with dynamic regions of the cortical actin cytoskeleton in response to Rac1 activation. *Mol Biol Cell* **11**, 393–412.
 - 21 Wolf K, Wu YI, Liu Y, Geiger J, Tam E, Overall C, Stack MS & Friedl P (2007) Multi-step pericellular proteolysis controls the transition from individual to collective cancer cell invasion. *Nat Cell Biol* **9**, 893–904.
 - 22 Branch KM, Hoshino D & Weaver AM (2012) Adhesion rings surround invadopodia and promote maturation. *Biol Open* **1**, 711–722.
 - 23 Pignatelli J, Tumbarello DA, Schmidt RP & Turner CE (2012) Hic-5 promotes invadopodia formation and invasion during TGF-beta-induced epithelial-mesenchymal transition. *J Cell Biol* **197**, 421–437.
 - 24 Burridge K & Feramisco JR (1980) Microinjection and localization of a 130K protein in living fibroblasts: a relationship to actin and fibronectin. *Cell* **19**, 587–595.
 - 25 Bakolitsa C, Cohen DM, Bankston LA, Bobkov AA, Cadwell GW, Jennings L, Critchley DR, Craig SW & Liddington RC (2004) Structural basis for vinculin activation at sites of cell adhesion. *Nature* **430**, 583–586.
 - 26 Humphries JD, Wang P, Streuli C, Geiger B, Humphries MJ & Ballestrem C (2007) Vinculin controls focal adhesion formation by direct interactions with talin and actin. *J Cell Biol* **179**, 1043–1057.
 - 27 Zaidel-Bar R & Geiger B (2010) The switchable integrin adhesome. *J Cell Sci* **123**, 1385–1388.
 - 28 Zaidel-Bar R, Milo R, Kam Z & Geiger B (2007) A paxillin tyrosine phosphorylation switch regulates the assembly and form of cell-matrix adhesions. *J Cell Sci* **120**, 137–148.
 - 29 Iozzo RV & Schaefer L (2015) Proteoglycan form and function: a comprehensive nomenclature of proteoglycans. *Matrix Biol* **42**, 11–55.
 - 30 Karamanos NK, Piperigkou Z, Theocharis AD, Watanabe H, Franchi M, Baud S, Brezillon S, Gotte M, Passi A, Vigetti D *et al.* (2018) Proteoglycan chemical diversity drives multifunctional cell regulation and therapeutics. *Chem Rev* **118**, 9152–9232.
 - 31 Theocharis AD, Skandalis SS, Gialeli C & Karamanos NK (2016) Extracellular matrix structure. *Adv Drug Deliv Rev* **97**, 4–27.
 - 32 Neill T, Schaefer L & Iozzo RV (2015) Decoding the matrix: instructive roles of proteoglycan receptors. *Biochemistry* **54**, 4583–4598.
 - 33 Karamanou K, Perrot G, Maquart FX & Brezillon S (2018) Lumican as a multivalent effector in wound healing. *Adv Drug Deliv Rev* **129**, 344–351.
 - 34 Pietraszek-Gremplewicz K, Karamanou K, Niang A, Dauchez M, Belloy N, Maquart FX, Baud S & Brezillon S (2019) Small leucine-rich proteoglycans and matrix metalloproteinase-14: key partners? *Matrix Biol* **75–76**, 271–285.
 - 35 Brezillon S, Pietraszek K, Maquart FX & Wegrowski Y (2013) Lumican effects in the control of tumour progression and their links with metalloproteinases and integrins. *FEBS J* **280**, 2369–2381.
 - 36 Chakravarti S & Magnuson T (1995) Localization of mouse lumican (keratan sulfate proteoglycan) to distal chromosome 10. *Mamm Genome* **6**, 367–368.
 - 37 Grover J, Chen XN, Korenberg JR & Roughley PJ (1995) The human lumican gene. Organization, chromosomal location, and expression in articular cartilage. *J Biol Chem* **270**, 21942–21949.
 - 38 Seomun Y & Joo CK (2008) Lumican induces human corneal epithelial cell migration and integrin expression

- via ERK 1/2 signaling. *Biochem Biophys Res Commun* **372**, 221–225.
- 39 Nikitovic D, Chalkiadaki G, Berdiaki A, Aggelidakis J, Katonis P, Karamanos NK & Tzanakakis GN (2011) Lumican regulates osteosarcoma cell adhesion by modulating TGFbeta2 activity. *Int J Biochem Cell Biol* **43**, 928–935.
- 40 Stasiak M, Boncela J, Perreau C, Karamanou K, Chatron-Colliet A, Prout I, Przygodzka P, Chakravarti S, Maquart FX, Kowalska MA *et al.* (2016) Lumican inhibits SNAIL-induced melanoma cell migration specifically by blocking MMP-14 activity. *PLoS ONE* **11**, e0150226.
- 41 Karamanou K, Franchi M, Piperigkou Z, Perreau C, Maquart FX, Vynios DH & Brezillon S (2017) Lumican effectively regulates the estrogen receptors-associated functional properties of breast cancer cells, expression of matrix effectors and epithelial-to-mesenchymal transition. *Sci Rep* **7**, 45138.
- 42 Garantziotis S & Savani RC (2019) Hyaluronan biology: a complex balancing act of structure, function, location and context. *Matrix Biol* **78–79**, 1–10.
- 43 Velesiotis C, Vasileiou S & Vynios DH (2019) A guide to hyaluronan and related enzymes in breast cancer: biological significance and diagnostic value. *FEBS J* **286**, 3057–3074.
- 44 Olsson E, Honeth G, Bendahl PO, Saal LH, Gruberger-Saal S, Ringner M, Vallon-Christersson J, Jonsson G, Holm K, Lovgren K *et al.* (2011) CD44 isoforms are heterogeneously expressed in breast cancer and correlate with tumor subtypes and cancer stem cell markers. *BMC Cancer* **11**, 418.
- 45 Hsu CP, Lee LY, Hsu JT, Hsu YP, Wu YT, Wang SY, Yeh CN, Chen TC & Hwang TL (2018) CD44 predicts early recurrence in pancreatic cancer patients undergoing radical surgery. *In Vivo* **32**, 1533–1540.
- 46 Hiraga T, Ito S & Nakamura H (2013) Cancer stem-like cell marker CD44 promotes bone metastases by enhancing tumorigenicity, cell motility, and hyaluronan production. *Cancer Res* **73**, 4112–4122.
- 47 Yae T, Tsuchihashi K, Ishimoto T, Motohara T, Yoshikawa M, Yoshida GJ, Wada T, Masuko T, Mogushi K, Tanaka H *et al.* (2012) Alternative splicing of CD44 mRNA by ESRP1 enhances lung colonization of metastatic cancer cell. *Nat Commun* **3**, 883.
- 48 Poukka M, Bykachev A, Siiskonen H, Tynnela-Korhonen K, Auvinen P, Pasonen-Seppanen S & Sironen R (2016) Decreased expression of hyaluronan synthase 1 and 2 associates with poor prognosis in cutaneous melanoma. *BMC Cancer* **16**, 313.
- 49 Twarock S, Tammi MI, Savani RC & Fischer JW (2010) Hyaluronan stabilizes focal adhesions, filopodia, and the proliferative phenotype in esophageal squamous carcinoma cells. *J Biol Chem* **285**, 23276–23284.
- 50 Rilla K, Siiskonen H, Tammi M & Tammi R (2014) Hyaluronan-coated extracellular vesicles – a novel link between hyaluronan and cancer. *Adv Cancer Res* **123**, 121–148.
- 51 Vuillermoz B, Khoruzhenko A, D’Onofrio MF, Ramont L, Venteo L, Perreau C, Antonicelli F, Maquart FX & Wegrowski Y (2004) The small leucine-rich proteoglycan lumican inhibits melanoma progression. *Exp Cell Res* **296**, 294–306.
- 52 Zeltz C, Brezillon S, Kapyla J, Eble JA, Bobichon H, Terryn C, Perreau C, Franz CM, Heino J, Maquart FX *et al.* (2010) Lumican inhibits cell migration through alpha2beta1 integrin. *Exp Cell Res* **316**, 2922–2931.
- 53 D’Onofrio MF, Brezillon S, Baranek T, Perreau C, Roughley PJ, Maquart FX & Wegrowski Y (2008) Identification of beta1 integrin as mediator of melanoma cell adhesion to lumican. *Biochem Biophys Res Commun* **365**, 266–272.
- 54 Zutter MM, Santoro SA, Staatz WD & Tsung YL (1995) Re-expression of the alpha 2 beta 1 integrin abrogates the malignant phenotype of breast carcinoma cells. *Proc Natl Acad Sci USA* **92**, 7411–7415.
- 55 Desgrosellier JS, Lesperance J, Seguin L, Gozo M, Kato S, Franovic A, Yebra M, Shattil SJ & Cheresch DA (2014) Integrin alphavbeta3 drives slug activation and stemness in the pregnant and neoplastic mammary gland. *Dev Cell* **30**, 295–308.
- 56 Bockhorn M, Roberge S, Sousa C, Jain RK & Munn LL (2004) Differential gene expression in metastasizing cells shed from kidney tumors. *Cancer Res* **64**, 2469–2473.
- 57 Margadant C, Raymond K, Kreft M, Sachs N, Janssen H & Sonnenberg A (2009) Integrin alpha3beta1 inhibits directional migration and wound re-epithelialization in the skin. *J Cell Sci* **122**, 278–288.
- 58 Carter WG, Kaur P, Gil SG, Gahr PJ & Wayner EA (1990) Distinct functions for integrins alpha 3 beta 1 in focal adhesions and alpha 6 beta 4/bullous pemphigoid antigen in a new stable anchoring contact (SAC) of keratinocytes: relation to hemidesmosomes. *J Cell Biol* **111**, 3141–3154.
- 59 Stipp CS (2010) Laminin-binding integrins and their tetraspanin partners as potential antimetastatic targets. *Expert Rev Mol Med* **12**, e3.
- 60 Ren B, O’Brien BA, Swan MA, Koina ME, Nassif N, Wei MQ & Simpson AM (2007) Long-term correction of diabetes in rats after lentiviral hepatic insulin gene therapy. *Diabetologia* **50**, 1910–1920.
- 61 Vuori K, Hirai H, Aizawa S & Ruoslahti E (1996) Introduction of p130cas signaling complex formation upon integrin-mediated cell adhesion: a role for Src family kinases. *Mol Cell Biol* **16**, 2606–2613.
- 62 Fassler R & Meyer M (1995) Consequences of lack of beta 1 integrin gene expression in mice. *Genes Dev* **9**, 1896–1908.

- 63 Holtkotter O, Nieswandt B, Smyth N, Muller W, Hafner M, Schulte V, Krieg T & Eckes B (2002) Integrin alpha 2-deficient mice develop normally, are fertile, but display partially defective platelet interaction with collagen. *J Biol Chem* **277**, 10789–10794.
- 64 Nikitovic D, Chatzinikolaou G, Tsiaoussis J, Tsatsakis A, Karamanos NK & Tzanakakis GN (2012) Insights into targeting colon cancer cell fate at the level of proteoglycans/glycosaminoglycans. *Curr Med Chem* **19**, 4247–4258.
- 65 Nikitovic D, Katonis P, Tsatsakis A, Karamanos NK & Tzanakakis GN (2008) Lumican, a small leucine-rich proteoglycan. *IUBMB Life* **60**, 818–823.
- 66 Brezillon S, Radwanska A, Zeltz C, Malkowski A, Ploton D, Bobichon H, Perreau C, Malicka-Blaszkiewicz M, Maquart FX & Wegrowski Y (2009) Lumican core protein inhibits melanoma cell migration via alterations of focal adhesion complexes. *Cancer Lett* **283**, 92–100.
- 67 Ishiwata T, Yamamoto T, Kawahara K, Kawamoto Y, Matsuda Y, Ishiwata S & Naito Z (2010) Enhanced expression of lumican inhibited the attachment and growth of human embryonic kidney 293 cells. *Exp Mol Pathol* **88**, 363–370.
- 68 Radwanska A, Baczynska D, Nowak D, Brezillon S, Popow A, Maquart FX, Wegrowski Y & Malicka-Blaszkiewicz M (2008) Lumican affects actin cytoskeletal organization in human melanoma A375 cells. *Life Sci* **83**, 651–660.
- 69 Neill T, Schaefer L & Iozzo RV (2012) Decorin: a guardian from the matrix. *Am J Pathol* **181**, 380–387.
- 70 Piperigkou Z, Franchi M, Gotte M & Karamanos NK (2017) Estrogen receptor beta as epigenetic mediator of miR-10b and miR-145 in mammary cancer. *Matrix Biol* **64**, 94–111.
- 71 Rutnam ZJ, Wight TN & Yang BB (2013) miRNAs regulate expression and function of extracellular matrix molecules. *Matrix Biol* **32**, 74–85.
- 72 Kurozumi S, Yamaguchi Y, Kurozumi M, Ohira M, Matsumoto H & Horiguchi J (2017) Recent trends in microRNA research into breast cancer with particular focus on the associations between microRNAs and intrinsic subtypes. *J Hum Genet* **62**, 15–24.
- 73 Chang CJ, Hsu CC, Chang CH, Tsai LL, Chang YC, Lu SW, Yu CH, Huang HS, Wang JJ, Tsai CH *et al.* (2011) Let-7d functions as novel regulator of epithelial-mesenchymal transition and chemoresistant property in oral cancer. *Oncol Rep* **26**, 1003–1010.
- 74 Thomson DW, Bracken CP, Szubert JM & Goodall GJ (2013) On measuring miRNAs after transient transfection of mimics or antisense inhibitors. *PLoS ONE* **8**, e55214.
- 75 Gregory PA, Bracken CP, Bert AG & Goodall GJ (2008) MicroRNAs as regulators of epithelial-mesenchymal transition. *Cell Cycle* **7**, 3112–3118.
- 76 Bai JX, Yan B, Zhao ZN, Xiao X, Qin WW, Zhang R, Jia LT, Meng YL, Jin BQ, Fan DM *et al.* (2013) Tamoxifen represses miR-200 microRNAs and promotes epithelial-to-mesenchymal transition by up-regulating c-Myc in endometrial carcinoma cell lines. *Endocrinology* **154**, 635–645.
- 77 Albin A (2016) Extracellular matrix invasion in metastases and angiogenesis: commentary on the matrigel “chemoinvasion assay”. *Cancer Res* **76**, 4595–4597.
- 78 Sato K, Matsuda H & Sasaki A (1994) Pathogen invasion and host extinction in lattice structured populations. *J Math Biol* **32**, 251–268.
- 79 Rochefort H, Platet N, Hayashido Y, Derocq D, Lucas A, Cunat S & Garcia M (1998) Estrogen receptor mediated inhibition of cancer cell invasion and motility: an overview. *J Steroid Biochem Mol Biol* **65**, 163–168.